Scripta Materialia 123 (2016) 34–37

Contents lists available at ScienceDirect

Scripta Materialia

journal homepage: www.elsevier.com/locate/scriptamat

Regular Article

Structural and mechanical properties of nitrogen-deficient cubic Cr–Mo–N and Cr–W–N systems

Liangcai Zhou [a], Fedor F. Klimashin [a], David Holec [b], Paul H. Mayrhofer [a,*]

[a] Institute of Materials Science and Technology, Technische Universität Wien, Vienna, Austria
[b] Department of Physical Metallurgy and Materials Testing, Montanuniversität Leoben, Leoben, Austria

ARTICLE INFO

Article history:
Received 16 February 2016
Received in revised form 27 April 2016
Accepted 27 May 2016
Available online 7 June 2016

Keywords:
Cr–Mo–N and Cr–W–N
Vacancy
First-principles
Mechanical properties
Phase stability

ABSTRACT

Our computational and experimental results reveal the inherent driving force of cubic Cr–TM–N (TM = Mo, W) solid solutions for nitrogen deficiency, expressed chemically as $Cr_{1-x}TM_xN_{1-0.5x}$. Their computationally predicted large positive mixing enthalpies indicate a high driving force for isostructural decomposition into B1-structured CrN and γ-TM_2N. The calculations further predict an improved ductility with increasing TM-content and significant anisotropy of elastic constants and Young's modulus in the entire compositional range. The experimentally measured lattice parameters, nitrogen content in Cr-Mo-N, and elastic properties of $Cr_{1-x}TM_xN_{1-0.5x}$ corroborated our theoretical predictions. Our combined theoretical and experimental study provides new understanding and insights into these complex material systems.

The paramagnetic chromium nitride (CrN) with cubic B1 structure (NaCl prototype, space group $Fm\bar{3}m$) is one of the most important transitional metal nitrides, and not just used as a protective coating due to its superior wear, corrosion and oxidation resistance [1]. In order to further tune the structural, mechanical, and tribological properties to diverse service conditions, alloying with other elements has proven to be an effective concept [2–4]. Specifically, alloying molybdenum (Mo) or tungsten (W) into CrN coatings has been confirmed to be effective to improve the tribological properties [2,3]. The ability of Mo and W to form Magnéli phase oxides can be used to prepare self-lubricant materials with a significantly reduced coefficient of friction [2,4].

The present work is also motivated by the controversial results in literature. Recently, Quintela et al. [5] pointed out that even very small additions of only ~1 at.% of Mo or W to CrN, lead to a spontaneous phase segregation into Mo- or W-rich regions. Contrary, Kwang et al. [3] stated that cubic Cr–Mo–N coatings with Mo content less than 30.4 at.% are a substitutional solid solution of (Cr, Mo)N. Recently we showed, that ternary Cr–Mo–N coatings can be prepared in single-phase B1 structure along the entire Mo_2N–CrN tie line [6]. Here, γ-TM_2N (TM = Mo, W) is a B1-like structure with half-filled N-sublattice [7]. The controversy can be explained by the fact that even the non-miscible compounds can form a solid solution when using non-equilibrium synthesis technique as, for instance, physical vapor deposition.

Although the cubic binary nitrides B1-MoN and B1-WN are mechanically unstable [8], they are often used as the boundary systems for cubic B1-(Cr, TM)N with nitrogen contents of constantly 50 at.%, as reported [3,9]. However, the significant deviation for the lattice parameters of cubic $Cr_{1-x}TM_xN$ between theoretical and experimental data in our previous work [10] also suggests that the vacancies in these cubic $Cr_{1-x}TM_xN$ solid solutions play an indispensable and significant role. In order to clarify these controversies, we have performed a comprehensive investigation on understoichiometric cubic $Cr_{1-x}Mo_xN_y$ and $Cr_{1-x}W_xN_y$ solid solutions by the evaluation of the structural and mechanical properties using first-principles calculations. The results are compared with experimentally obtained lattice parameters of sputter deposited $Cr_{1-x}Mo_xN_y$ coatings.

Density Functional Theory (DFT) based calculations are performed using the Vienna Ab initio Simulation Package (VASP) [11,12]. The ion-electron interactions are described by the projector augmented wave method (PAW) [13], and the generalized gradient approximation (GGA) as parameterized by Perdew–Burke–Ernzerhof (PBE) [14] is employed for the exchange-correction effects. In order to simulate the chemical disorder between Cr and TM atoms (here Mo and W) on the metal sublattice of the cubic B1 structure, and also the paramagnetic state induced by Cr atoms, we used the Special Quasi-random Structures (SQS) approach [15] as implemented and tested in our previous studies of CrN-based systems [10,16,17]. The content of nitrogen vacancies is treated as a linear dependence on the Mo or W content, basically to follow the quasi-binary CrN–TM_2N tie line. Hence, the chemical composition of cubic $(Cr,TM)N_y$ solid solutions can be described with $Cr_{1-x}TM_xN_{1-0.5x}$. We used $2 \times 2 \times 2$ supercells containing 64 atoms for the $Cr_{1-x}TM_xN_{1-0.5x}$ calculations, with Monkhorst-Pack grids [18] of $5 \times 5 \times 5$ *k*-point mesh. The short range order parameters

* Corresponding author.
E-mail address: paul.mayrhofer@tuwien.ac.at (P.H. Mayrhofer).

http://dx.doi.org/10.1016/j.scriptamat.2016.05.036

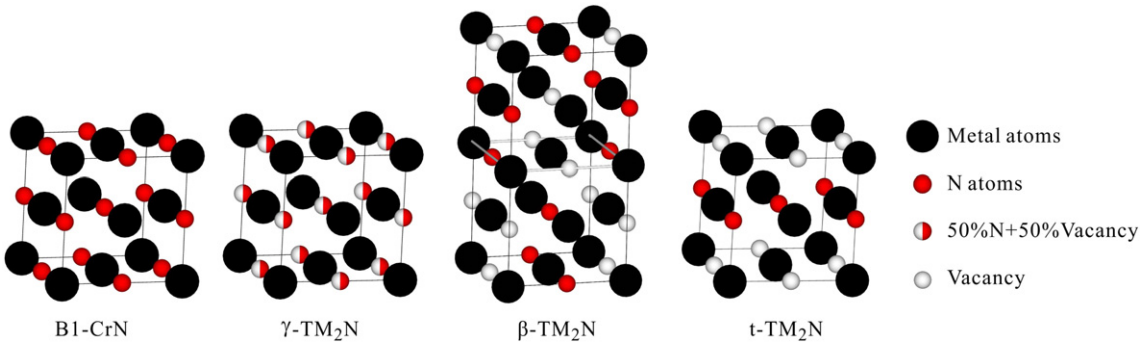

Fig. 1. Crystallographic structures of cubic B1-CrN, γ-TM_2N, β-TM_2N, and t-TM_2N.

(SROs) are optimized for pairs at least up to the fifth coordination shell. All calculations were performed with plane wave cutoff energy of 500 eV. Elastic properties of $Cr_{1-x}TM_xN_{1-0.5x}$ were evaluated by the stress-strain method [10,16].

All coatings were deposited using a modified Leybold Heraeus Z400 DC magnetron sputtering system, for more details see Ref. [6]. In order to vary the chemical composition, cubes of Cr (99.99% purity, $3 \times 3 \times 3$ mm) were uniformly arranged on the race track of a Mo target (99.99% purity and 75 mm in diameter), and reactively sputtered in a mixed N_2/Ar atmosphere (both with 99.999% purity) onto single crystal silicon (100) and austenite substrates. Before the deposition, the chamber was evacuated to a high vacuum of $5 \cdot 10^{-4}$ Pa. All depositions were prepared at constant total pressure of 0.35 Pa (N_2-to-toal pressure ratio of 0.44), with DC target current of 0.4 A, floating potential of the substrates of −15 V, and a substrate temperature of 450 ± 20 °C. Phase analyses were performed using an X-ray diffractometer in the Bragg-Brentano geometry with a monochromized Cu K_α radiation, the lattice constants were consequently obtained by fitting the peak positions in the diffraction patterns. Elemental composition was determined by means of energy dispersive X-ray spectroscopy and calibrated using Mo–N and Mo–Cr–N thin film standards characterized by elastic recoil detection analysis. The film-only indentation moduli were measured with a nanoindentor using a Berkovich diamond tip within the load range 3–30 mN and an evaluation procedure according to Oliver and Pharr [19] as described in detail in Refs. [6,20].

Fig. 1 presents the crystal structures of cubic B1-CrN, γ-TM_2N (TM = Mo, W), β-TM_2N, and t-TM_2N. γ-TM_2N has a defective cubic B1 structure with 50% disordered vacancies in the nitrogen sublattice [7]. β-TM_2N (space group $I4_1/amd$) is a low-temperature tetragonal phase with an ordering of vacancies on the non-metal sublattice from γ-TM_2N [21]. Tetragonal t-Mo_2N is constructed from perfect cubic B1-TMN by removing 50% of the nitrogen atoms in the [100] and [010] directions in order to obtain 50% vacancies on the non-metal sublattice [22]. Three different structural configurations are tested for γ-TM_2N and the results are listed in Table 1, where γ-$TM_{32}N_{16}$ denotes the SQS configuration. It clearly shows that the different structural configurations only little influence the total energies, lattice parameters, and bulk moduli, therefore they are not further considered here. Especially, the experimental bulk moduli and the lattice parameters of γ-TM_2N [23,24] show an excellent agreement with calculated results.

The nitrogen content within our sputter deposited Cr–Mo–N coatings strongly depends on their Mo content, see Fig. 2a. The experimental data nicely follow our calculated model solid solutions $Cr_{1-x}TM_xN_{1-0.5x}$, where the nitrogen content decreases (due to increasing amount of N-vacancies at the nitrogen sublattice) with increasing Mo or W content. Consequently, nitrogen vacancies need to be addressed for these material systems. The calculated lattice parameters of stoichiometric cubic $Cr_{1-x}TM_xN$ show a significant deviation from experimental data [7,25–28] and the deviation increases with increasing Mo or W content [10], see Fig. 2b. On the other hand, the calculated results for cubic $Cr_{1-x}TM_xN_{1-0.5x}$ with Mo- or W-dependent N vacancies, which are very similar, yield an excellent agreement with the experimental results and show a linear Vegard-like behavior [29]. This indicates that the nitrogen content in the cubic Cr–Mo–N and Cr–W–N solid solutions is linearly dependent on the fraction of γ-Mo_2N or γ-W_2N and hence varies along the CrN–TM_2N tie line, which has recently been confirmed by an independent experimental work [6].

We propose the chemical description with $Cr_{1-x}TM_xN_{1-0.5x}$ for single-phase face centered cubic Cr–Mo–N and Cr–W–N solid solutions. Here we want to mention that under some extreme conditions, it is possible to prepare single-phase face centered cubic $Cr_{1-x}Mo_xN$ or $Cr_{1-x}W_xN$ materials, but only up to a very limited maximum Mo or W content, and only when using a very high N_2 pressure during deposition [6]. While the theoretical and experimental lattice constants yield an excellent agreement for $Cr_{1-x}Mo_xN_{1-0.5x}$, the experimental lattice constants of $Cr_{1-x}W_xN_{1-0.5x}$ show a small positive deviation from the theoretical results, which is more likely due to the excessive nitrogen atoms at the grain boundaries for overstoichiometric WN_x thin films [23]. Previous theoretical calculations have illustrated that the mixing enthalpies of $Cr_{1-x}TM_xN$ with respect to cubic B1-CrN and TMN are in contrast with experimental observations [10], and thus cannot be used to evaluate the phase stability of cubic Cr–Mo–N and Cr–W–N systems. In an earlier work, we have argued that this is because cubic B1-MoN and B1-WN are mechanically unstable, and therefore lead to the anomalous negative mixing enthalpies [10]. Therefore, we have suggested that using CrN + TM_2N + N_2 as the reference state for evaluating the mixing enthalpies of $Cr_{1-x}TM_xN$ is more meaningful [10]. Although the mixing enthalpies of $Cr_{1-x}TM_xN$, when using CrN + TM_2N + N_2 as the reference state, predict the possibility of isostructural decomposition, the description is not really correct, as the large substoichiometry of nitrogen in Cr–Mo–N and Cr–W–N solid solutions is not taken into account. Therefore, in addition to our previous studies also the mixing enthalpies of cubic $Cr_{1-x}Mo_xN_{1-0.5x}$ and $Cr_{1-x}W_xN_{1-0.5x}$ are evaluated with respect to cubic B1-CrN and γ-TM_2N (Fig. 3a), i.e., corresponding to the quasi-binary tie lines CrN–Mo_2N and CrN–W_2N, respectively.

Table 1
Calculated total energy, E_{total}, lattice parameters, a and c, volume per atom, V, bulk modulus, B, and the experimental data.

		γ-$Mo_{32}N_{16}$	β-Mo_2N	t-Mo_2N	γ-Mo_2N	γ-$W_{32}N_{16}$	β-W_2N	t-W_2N	γ-W_2N
- E_{total} (eV/at)		10.213	10.248	10.191	–	11.472	11.481	11.406	–
Lattice parameters (Å)	a	4.19	4.27	4.22	4.16 [7]	4.20	4.30	4.22	4.19 [23]
	c	–	8.04	4.18	–	–	7.98	4.19	–
V (Å^3/at)		12.26	12.26	12.44	12.00 [7]	12.35	12.35	12.53	12.26 [23]
B (GPa)		298	288	303	301 [24]	346	340	340	–

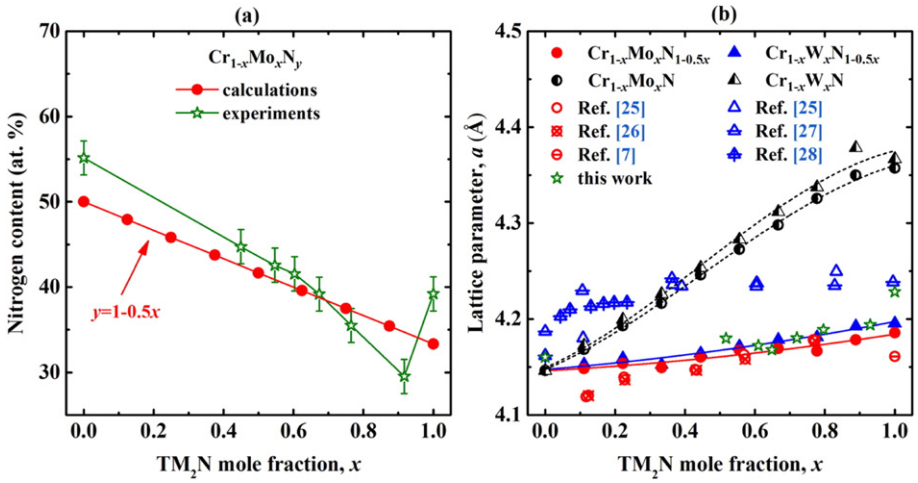

Fig. 2. (a) The nitrogen content (at.%) of deposited $Cr_{1-x}Mo_xN_y$ thin films (open symbols) as a function of their Mo-content, x, and the nitrogen compositions used in the calculations (solid symbols). (b) The ab initio obtained lattice parameters of vacancy-free B1-$Cr_{1-x}TM_xN$ (half-open symbols) and N-vacancy containing $Cr_{1-x}TM_xN_{1-0.5x}$ (solid symbols) as a function of their TM-fraction on metal sublattice, and reference values (open symbols with the highlighted trends).

Although our data explicitly address only certain content of nitrogen vacancies (corresponding to the $Cr_{1-x}TM_xN_{1-0.5x}$ chemical formula), they represent the lower limit of the mixing enthalpies of cubic $Cr_{1-x}Mo_xN_{1-y}$ (with $y < 0.5x$). The large positive mixing enthalpies for $Cr_{1-x}Mo_xN_{1-0.5x}$ and $Cr_{1-x}W_xN_{1-0.5x}$ are comparable to the well-investigated $Ti_{1-x}Al_xN$ system with a maximum mixing enthalpy of about 0.11 eV/atom. The $Ti_{1-x}Al_xN$ system is well investigated and experiences a spinodal decomposition into coherent Al- and Ti-enrich cubic domains [30]. This implies that cubic Cr–Mo–N and Cr–W–N systems show great tendency towards isostructural phase decomposition. Hence, by near-equilibrium deposition techniques it will be difficult to synthesize single-phase cubic $Cr_{1-x}Mo_xN_{1-0.5x}$ and $Cr_{1-x}W_xN_{1-0.5x}$ solid solutions. This is consistent with recent experimental observations, showing that even for the lowest concentrations (~1 at.%), spontaneous phase segregation into Mo- and W-rich regions occurs [5]. However, by physical vapor deposition, especially when using only moderate substrate temperatures (below 0.3 of the melting point of the prepared coating), solid solutions far from the thermodynamic equilibrium (i.e., metastable and even thermodynamically unstable) can be realized [31]. The calculated elastic constants C_{11}, C_{12}, and C_{44}, for cubic $Cr_{1-x}Mo_xN_{1-0.5x}$ and $Cr_{1-x}W_xN_{1-0.5x}$ solid solutions (Fig. 3b), fulfill the corresponding Huang-Born stability criteria [32]. Consequently, cubic $Cr_{1-x}Mo_xN_{1-0.5x}$ and $Cr_{1-x}W_xN_{1-0.5x}$ are mechanically stable over the entire composition range. This is a further strong argument (in addition to the excellent agreement between calculated and measured nitrogen content and the calculated mixing enthalpy), that for these material systems the content of nitrogen vacancies scales with the Mo or W content, hence following the chemical formula $Cr_{1-x}TM_xN_{1-0.5x}$. The calculated elastic constant C_{12} increases with the content of γ-TM_2N, while C_{44} keeps an almost constant value in the whole composition range. Hence, our calculated elastic constants suggest $C_{12} > C_{44}$ within the whole range of TM_2N mole fraction, and the difference becomes even more pronounced with increasing TM_2N mole fraction. Pettifor [33] suggested that the Cauchy pressure, C_{12}-C_{44}, should be positive for ductile materials. This empirical criterion was verified, e.g., by Niu *et al.* for many cubic-structured materials [34]. Consequently, with increasing Mo or W content the ductility of $Cr_{1-x}TM_xN_{1-0.5x}$ is expected to increase.

Deposited thin films usually have a fibre texture with a preferred orientation along a certain ⟨*hkl*⟩ direction perpendicular to the substrate surface [35]. Therefore, we calculated directionally dependent single crystal Young's moduli, E_{hkl}, for cubic $Cr_{1-x}Mo_xN_{1-0.5x}$ and $Cr_{1-x}W_xN_{1-0.5x}$ compositions in ⟨100⟩, ⟨110⟩, and ⟨111⟩ directions, Fig. 4a, b. These are discussed as extreme values for fibre-textured microstructures, as explicitly shown in Ref. [36]. Both cubic solid solutions, $Cr_{1-x}Mo_xN_{1-0.5x}$

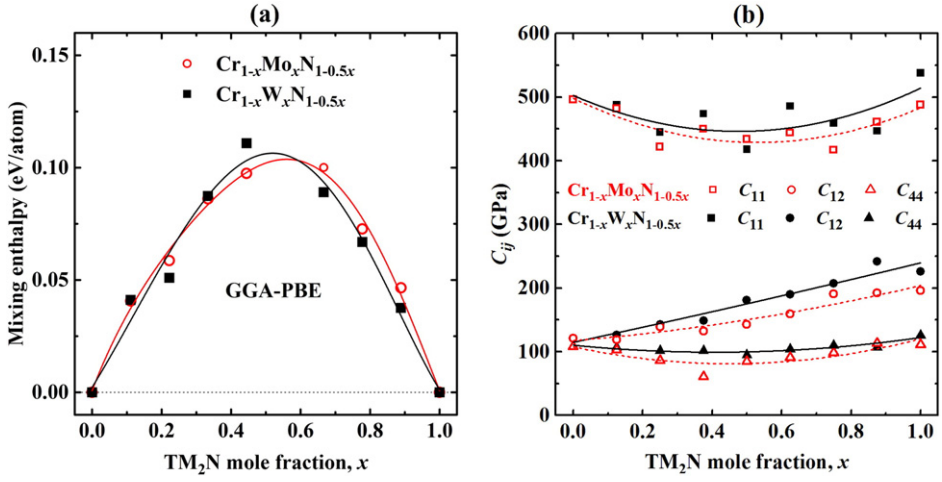

Fig. 3. (a) Calculated isostructural mixing enthalpies of B1-$Cr_{1-x}Mo_xN_{1-0.5x}$ (red open circles) and B1-$Cr_{1-x}W_xN_{1-0.5x}$ (black solid squares) as functions of TM_2N-content. (b) Calculated single crystal elastic constants C_{11}, C_{12}, and C_{44} of B1-$Cr_{1-x}TM_xN_{1-0.5x}$.

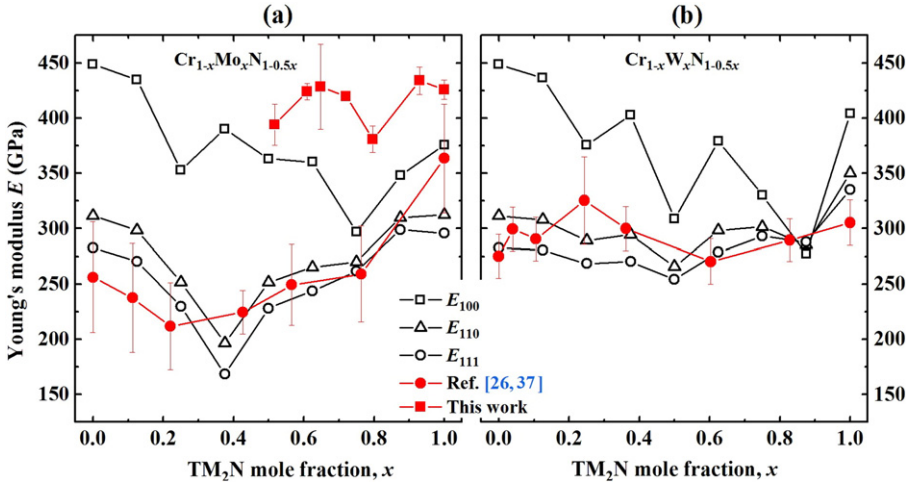

Fig. 4. Predicted Young's moduli in the ⟨100⟩ (open squares), ⟨110⟩ (open triangles), ⟨111⟩ (open circles) directions of B1-$Cr_{1-x}TM_xN_{1-0.5x}$ – TM = Mo (a), W (b) – as functions of their TM_2N-content compared with experimental data (solid symbols).

and $Cr_{1-x}W_xN_{1-0.5x}$, exhibit directionally dependent Young's moduli in the whole composition range, with ⟨100⟩ direction being significantly stiffer than the other directions. This behavior follows the single crystal elastic constant C_{ij}, Fig. 4a, due to the strongest contribution of C_{11} to E_{100} . The calculated E_{100} data are in excellent agreement to the experimentally obtained indentation moduli of our coatings with a strong ⟨100⟩ growth texture. The reported indentation moduli of coatings with a preferred ⟨111⟩ orientation [26,37] are in excellent agreement with our E_{111} calculations. Our data clearly show that the Young's moduli can be significantly different for various directions, though the agreement of absolute values is likely to be coincidental due to development of complex deformation during indentation loading. Nevertheless, we clearly show that texture needs to be considered when comparing experimental and theoretical data [36].

In summary, the nitrogen substoichiometry in cubic Cr–Mo–N and Cr–W–N solid solutions was systemically studied by first-principles calculations and compared with experimental data of the lattice spacing, composition, and elastic properties. Cubic Cr–Mo–N and Cr–W–N systems intrinsically contain a significant amount of vacancies on the N sublattice that can best be described using the chemical formula $Cr_{1-x}TM_xN_{1-0.5x}$, rather than the conventionally used $Cr_{1-x}TM_xN$. The ab initio predicted large positive mixing enthalpies of cubic $Cr_{1-x}Mo_xN_{1-0.5x}$ and $Cr_{1-x}W_xN_{1-0.5x}$ indicate a significant thermodynamic driving force for isostructural phase decomposition into cubic B1-CrN and γ-TM_2N. The calculated elastic constants further suggest the cubic $Cr_{1-x}Mo_xN_{1-0.5x}$ and $Cr_{1-x}W_xN_{1-0.5x}$ solid solutions being mechanically stable within the whole compositional range, and the positive Cauchy pressure, C_{12}-C_{44}, indicates increasing ductility with increasing Mo or W content. Furthermore, our calculated Young's moduli – yielding considerably stiffer behavior along the ⟨100⟩ direction than in the ⟨110⟩ or ⟨111⟩ directions – are in excellent agreement with the indentation moduli measured on the (200) predominantly oriented $Cr_{1-x}Mo_xN_{1-0.5x}$ coatings as well as with reported experimental data from literature, thus underlying the importance of texture on the overall mechanical response of the coatings.

Acknowledgements

The financial support by the START Program (Y371) of the Austrian Science Fund (FWF) is gratefully acknowledged. The computational results presented have been achieved using the Vienna Scientific Cluster (VSC).

References

[1] G. Berg, C. Friedrich, E. Broszeit, C. Berger, Surf. Coat. Technol. 86 (1996) 184–191.
[2] B. Gu, J.P. Tu, X.H. Zheng, Y.Z. Yang, S.M. Peng, Surf. Coat. Technol. 202 (2008) 2189–2193.
[3] K. Ho Kim, E. Young Choi, S. Gyun Hong, B. Gyu Park, J. Hong Yoon, J. Hae Yong, Surf. Coat. Technol. 201 (2006) 4068–4072.
[4] G. Gassner, P.H. Mayrhofer, K. Kutschej, C. Mitterer, M. Kathrein, Surf. Coat. Technol. 201 (2006) 3335–3341.
[5] C.X. Quintela, B. Rodríguez-González, F. Rivadulla, Appl. Phys. Lett. 104 (2014) 022103.
[6] F.F. Klimashin, H. Riedl, D. Primetzhofer, J. Paulitsch, P.H. Mayrhofer, J. Appl. Phys. 118 (2015) 55–61.
[7] C.L. Bull, T. Kawashima, P.F. McMillan, D. Machon, O. Shebanova, D. Daisenberger, E. Soignard, E. Takayama-Muromachi, L.C. Chapon, J. Solid State, Chem. 179 (2006) 1762–1767.
[8] G.L.W. Hart, B.M. Klein, Phys. Rev. B 61 (2000) 3151–3154.
[9] F.-B. Wu, S.-K. Tien, J.-G. Duh, Surf. Coat. Technol. 200 (2005) 1514–1518.
[10] L. Zhou, D. Holec, P.H. Mayrhofer, J. Phys. D. Appl. Phys. 46 (2013) 365301.
[11] G. Kresse, J. Hafner, Phys. Rev. B 47 (1993) 558–561.
[12] G. Kresse, J. Furthmüller, Phys. Rev. B 54 (1996) 11169–11186.
[13] G. Kresse, D. Joubert, Phys. Rev. B 59 (1999) 1758–1775.
[14] J.P. Perdew, K. Burke, M. Ernzerhof, Phys. Rev. Lett. 77 (1996) 3865–3868.
[15] S.H. Wei, L.G. Ferreira, J.E. Bernard, A. Zunger, Phys. Rev. B 42 (1990) 9622–9649.
[16] L. Zhou, D. Holec, P.H. Mayrhofer, J. Appl. Phys. 113 (2013) 043511.
[17] L. Zhou, F. Körmann, D. Holec, M. Bartosik, B. Grabowski, J. Neugebauer, P.H. Mayrhofer, Phys. Rev. B 90 (2014) 184102.
[18] H.J. Monkhorst, J.D. Pack, Phys. Rev. B 13 (1976) 5188–5192.
[19] W.C. Oliver, G.M. Pharr, J. Mater. Res. 7 (1992) 1564–1580.
[20] A.C. Fischer-Cripps, Surf. Coat. Technol. 200 (2006) 4153–4165.
[21] P. Ettmayer, Monatsh. Chem. 101 (1970) 127–140.
[22] I. Matanović, F.H. Garzon, N.J. Henson, Phys. Chem. Chem. Phys. 16 (2014) 3014–3026.
[23] Y.G. Shen, Y.W. Mai, Mater. Sci. Eng. A 288 (2000) 47–53.
[24] E. Soignard, P.F. McMillan, T.D. Chaplin, S.M. Farag, C.L. Bull, M.S. Somayazulu, K. Leinenweber, Phys. Rev. B 68 (2003) 132101.
[25] P. Hones, R. Sanjinés, F. Lévy, Thin Solid Films 332 (1998) 240–246.
[26] P. Hones, R. Sanjinés, F. Lévy, O. Shojaei, J. Vac, A 17 (1999) 1024–1030.
[27] P. Hones, M. Diserens, R. Sanjinés, F. Lévy, J. Vac, B 18 (2000) 2851–2856.
[28] B.S. Yau, C.W. Chu, D. Lin, W. Lee, J.G. Duh, C.H. Lin, Thin Solid Films 516 (2008) 1877–1882.
[29] L. Vegard, Z. Phys. 5 (1921) 17–26.
[30] D. Holec, R. Rachbauer, L. Chen, L. Wang, D. Luef, P.H. Mayrhofer, Surf. Coat. Technol. 206 (2011) 1698–1704.
[31] P.H. Mayrhofer, C. Mitterer, L. Hultman, H. Clemens, Prog. Mater. Sci. 51 (2006) 1032–1114.
[32] M. Born, K. Huang, G. Britain, Dynamical Theory of Crystal Lattices, Clarendon Press Oxford, 1954.
[33] D. Pettifor, Mater. Sci. Technol. 8 (1992) 345–349.
[34] H. Niu, X.-Q. Chen, P. Liu, W. Xing, X. Cheng, D. Li, Y. Li, Scientific Reports, 2, 2012.
[35] K.J. Martinschitz, R. Daniel, C. Mitterer, J. Keckes, J. Appl. Crystallogr. 42 (2009) 416–428.
[36] D. Holec, F. Tasnádi, P. Wagner, M. Friák, J. Neugebauer, P.H. Mayrhofer, J. Keckes, Phys. Rev. B 90 (2014) 184106.
[37] F. Lévy, P. Hones, P.E. Schmid, R. Sanjinés, M. Diserens, C. Wiemer, Surf. Coat. Technol. 120-121 (1999) 284–290.